Chapter 5

# Classical Density Functional Theory for Fluids Adsorption in MOFs

Yu Liu and Honglai Liu

Additional information is available at the end of the chapter

http://dx.doi.org/10.5772/64632

**Abstract**

The designing of metal organic frameworks (MOFs) requires an efficient method to predict its adsorption properties. The conventional method to do this is molecular simulation, which is time consuming. In contrast, classical density functional theory (CDFT) is a much more efficient tool. Recently, CDFT has been successfully applied to MOF adsorptions. In this chapter, we will introduce the development and the different versions of CDFT and show how to apply CDFT to predict fluid adsorption in MOFs. We have reviewed the recent applications of CDFT in MOF adsorption and mainly focused on material screening. According to the recent developments, it seems CDFT is an efficient and robust tool for material screening; how to deal with more complicated fluids is the challenge of current CDFT.

**Keywords:** classical density functional theory, fluids, material-screening, MOFs, thermodynamics

## 1. Introduction

Adsorption is one of the essential properties of MOF materials, to give an efficient prediction of which is an important issue in the designing and application of MOFs. The traditional method to do this is molecular simulation, which is time consuming and may not be the best choice in real applications [1–3]. Take the high-throughput screenings for example, the number of MOFs in a typical screening database is more than $10^5$; the typical computational time of MC simulation for each MOF is approximately 0.25 CPU hour; this means a screening time cost over $10^3$ CPU days, which is a waste of resources. In this case, a more efficient method is needed, and the CDFT seems to be a promising alternative.

CDFT is a thermodynamic-statistical mechanics theory for inhomogeneous fluids. The concept of CDFT originates from quantum density functional theory and was formed in the1970s [4, 5]. During the past 40 years, CDFT has been developed from simple fluids to polymers, from equilibrium to dynamic, from high symmetry modeling systems to real systems, and has revealed itself as an efficient and robust tool in various fields including adsorption, wetting, freezing, solvation, and so on [6–35].

The application of CDFT to MOF adsorption was first proposed by Siderius et al. [27] in 2009 and has been advanced by Liu et al. [26] subsequently. Siderius and Liu et al. have demonstrated that CDFT can be used to predict gas adsorption in MOFs. However, the numerical algorithm of these pioneered applications is too simple, which makes the computational cost of CDFT even higher than molecular simulations. Such disadvantage has been solved by Liu and Wu recently by applying the fast Fourier transform (FFT) and conjugate gradient (CG) descent method [31, 33, 35]. Now, the advanced CDFT is faster than conventional simulations by two orders of magnitude and has been successfully applied to high-throughput screening for material design [33–36].

In the rest of this chapter, we will introduce the classical density functional theory and show how to implement the theory to MOF adsorptions. The remainder of this chapter is organized as follows: Section 2 will introduce the theoretical framework of CDFT; Section 3 will show how to apply CDFT to MOF adsorption and review recent reports in this field; and finally, Section 4 will summarize and prospect the current and future applications of CDFT on MOF adsorption.

## 2. Classical density functional theory

### 2.1. Thermodynamic framework

The central idea of CDFT is to obtain the fluid's microscopic conformation (density profile) by minimizing the grand potential or free energy and obtain the macroscopic information (such as uptake, heat of adsorption, selectivity, etc.) from the density profile. The main task of this procedure is to represent the grand potential as a functional of density profile. According to the definition, grand potential can be written by:

$$\Omega[\rho(\mathbf{r})] = F[\rho(\mathbf{r})] - \mu \int \rho(\mathbf{r})\,\mathrm{d}\,\mathbf{r} \tag{1}$$

where $\Omega$ is the grand potential, $F$ is the free energy, $\rho(\mathbf{r})$ is the density profile and $\mu$ is the chemical potential, which can be obtained from the equilibrium condition

$$\mu = \mu_{\mathrm{b}} \tag{2}$$

where $\mu_b$ is the chemical potential of the bulk system which is in equilibrium with the inhomogeneous system. In statistical mechanics, the free energy, $F$, can be obtained from the Hamiltonian of the system. Generally, the Hamiltonian is given by:

$$H = \sum_{i=1}^{N} \frac{p_i^2}{2m} + V\left(\left\{\mathbf{r}_i\right\}\right) \tag{3}$$

where $\boldsymbol{p}_i$ is the momenta of molecule $i$, $m$ is the mass of the molecule, $N$ is the number of molecules, and $V$ is the potential, which can be expanded mathematically:

$$V\left(\left\{\mathbf{r}_i\right\}\right) = u^{(0)} + \sum_{i=1}^{N} u_i^{(1)}(\mathbf{r}_i) + \sum_{1\le i<j\le N} u_{ij}^{(2)}(\mathbf{r}_{ij}) + \dots \tag{4}$$

For fluid (guest) adsorption in a rigid MOF (host), the 0th order term $u^{(0)}$ represents the host-host interactions, which is a constant and can be eliminated by defining the zero potential point. The first order term $u^{(1)}$ is the one-body potential representing the host-guest interactions. The second order term represents the guest-guest interactions. By ignoring the high order terms in classical systems, there are three contributions in the Hamiltonian: the kinetic contribution, the host-guest interaction and the guest-guest interaction, corresponding to the three terms in the free energy, the ideal gas free energy $F^{\mathrm{id}}$, the external free energy $F^{\mathrm{ext}}$, and the excess free energy $F^{\mathrm{ex}}$:

$$F[\rho(\mathbf{r})] = F^{\mathrm{id}}[\rho(\mathbf{r})] + F^{\mathrm{ext}}[\rho(\mathbf{r})] + F^{\mathrm{ex}}[\rho(\mathbf{r})] \tag{5}$$

For simple fluids, the ideal term and the external term can be exactly derived from the statistical mechanics by:

$$F^{\mathrm{id}}[\rho(\mathbf{r})] = k_{\mathrm{B}}T\int \rho(\mathbf{r})\left[\ln \rho(\mathbf{r})\Lambda^3 - 1\right]\mathrm{d}\mathbf{r} \tag{6}$$

$$F^{\mathrm{ext}}[\rho(\mathbf{r})] = \int \rho(\mathbf{r})V^{\mathrm{ext}}(\mathbf{r})\mathrm{d}\mathbf{r} \tag{7}$$

where $k_{\mathrm{B}}$ is the Boltzmann constant, $T$ is the temperature, $\Lambda$ is the de Broglie wave length and $V^{\mathrm{ext}}(\mathbf{r})$ is the external potential, which can be calculated from the direct interaction between host-guest interacting sites:

$$V^{\mathrm{ext}}(\mathbf{r}) = \sum_{i\in\mathrm{host}} u_{i,\mathrm{guest}}(\mathbf{r} - \mathbf{r}_i) \tag{8}$$

where $\mathbf{r}_i$ is the coordinate of the host (MOF) atoms and the host-guest interacting potential $u_{i,\text{guest}}(\mathbf{r})$ can be formed by standard force field such as the universal force field (UFF) [37] and Dreiding force field [38].

In contrast, the exact form of the excess free energy functional $F^{\text{ex}}[\rho(\mathbf{r})]$ is unknown for most systems, and approximations are needed. The detailed expression and discussions of these approximations will be introduced in Section 2.2. Here, we just assume the expression of $F^{\text{ext}}[\rho(\mathbf{r})]$ has already been given, in this case, we can establish the grand potential functional from Eqs. (1), (5)–(7). According to the second law of thermodynamics, the grand potential of an open system should reach its minimum when in equilibrium, which can be mathematically written by:

$$\frac{\delta\Omega[\rho(\mathbf{r})]}{\delta\rho(\mathbf{r})} = 0 \tag{9}$$

Substituting Eqs. (1), (5)–(7) in (9), we have:

$$\rho(\mathbf{r}) = \frac{1}{\Lambda^3}\exp\left[\beta\mu - \beta V^{\text{ext}}(\mathbf{r}) - \frac{\delta\beta F^{\text{ex}}}{\delta\rho(\mathbf{r})}\right] \tag{10}$$

where $\beta = 1/(k_B T)$ . In principle, the density profile $\rho(\mathbf{r})$ can be solved from Eq. (10), and the macroscopic properties can be calculated from $\rho(\mathbf{r})$. For example, the uptake $N$ is given by:

$$N = \int \rho(\mathbf{r})\,\mathrm{d}\,\mathbf{r} \tag{11}$$

The simplest application of Eq. (10) is the ideal gas system, representing fluids at low density limit. For ideal gas, $F^{\text{ex}}=0$, Eq. (10) can be simplified as:

$$\rho(\mathbf{r}) = \frac{1}{\Lambda^3}\exp\left[\beta\mu - \beta V^{\text{ext}}(\mathbf{r})\right] \tag{12}$$

Applying Eq. (12) to bulk system, where $V^{\text{ext}}(\mathbf{r})=0$, we have:

$$\rho_{\text{b}} = \frac{1}{\Lambda^3}\exp(\beta\mu_{\text{b}}) \tag{13}$$

where $\rho_{\text{b}}$ is the corresponding bulk density. Substituting Eq. (2) and (13) in (12), we have:

$$\rho(\mathbf{r}) = \rho_{\mathrm{b}} \exp\left[-\beta V^{\mathrm{ext}}(\mathbf{r})\right] \tag{14}$$

Then, the adsorption isotherm is given by:

$$N = \rho_{\mathrm{b}} \int \exp\left[-\beta V^{\mathrm{ext}}(\mathbf{r})\right] \mathrm{d}\mathbf{r} \tag{15}$$

As $V^{\mathrm{ext}}(\mathbf{r})$ only depends on the host-guest interaction instead of the loading of the guest molecule, Eq. (15) leads to a linear adsorption isotherm, which is true at low density limit. Moreover, the slope of the isotherm is determined by $V^{\mathrm{ext}}(\mathbf{r})$, which means the adsorption at low loadings is correlated with the host-guest interaction. This conclusion is also consistent with Snurr et al.'s findings in their high-throughput screening [1, 2].

### 2.2. Excess free energy functional

Ideal gas system is valid only for low loading systems. For more complicated systems, we need to consider the excess free energy functional. The excess free energy originates from the guest-guest correlations, which is much more complicated than the ideal free energy and external free energy. How to approximate the excess free energy is the center of concern in most CDFT. Up to now, various approximations have been proposed and applied, such as fundamental measure theory (FMT), weighted density approximation (WDA), and functional expansion theory.

#### *2.2.1. Local density approximation (LDA)*

LDA is the simplest approximation for excess free energy, which is given by an integration of homogeneous fluids:

$$F_{\mathrm{LDA}}^{\mathrm{ex}} = \int f_{\mathrm{V}}^{\mathrm{ex}}(\rho(\mathbf{r}))\,\mathrm{d}\mathbf{r} \tag{16}$$

where $f_{\mathrm{V}}^{\mathrm{ex}}(\rho)$ is the excess free energy density (per volume) as a function of fluid density for homogeneous systems. The methodology of Eq. (16) comes from the thinking of calculus: the system is first separated into small units, d**r**; the fluid in each d**r** is assumed to be homogeneous; the total excess free energy is represented as the summation of each local excess free energy. Due to its simplicity, LDA has been widely used for both classical and quantum systems when the scheme of DFT has been proposed [39–41]. However, there is an obvious disadvantage of LDA: the correlations between different d**r** are abandoned. The extensiveness of free energy is invalid for systems at molecular level. Representing the total excess free energy as the summation of each part is an approximation, which is valid only when the fluctuation of $\rho(\mathbf{r})$ is weak, such as vapor-liquid interface. However, for MOF adsorption, the fluctuation of $\rho(\mathbf{r})$ is very strong, as the guest molecules are usually highly localized at the favorable adsorption sites, where $\rho(\mathbf{r})$ approaches the Dirac delta function $\delta(\mathbf{r}-\mathbf{r}_i)$. In this case, LDA is not a proper approximation.

### 2.2.2. Gradient approximation

Gradient approximation considers the inhomogeneity beyond LDA. One of the widely used forms of gradient approximation is the so-called square-gradient approximation (SGA), which is derived from Ginzburg-Landau theory or Landau expansion [4, 5]:

$$F_{\mathrm{SGA}}^{\mathrm{ex}}\left[\rho(\mathbf{r})\right]=\int \mathrm{d}\mathbf{r}\left\{f^{\mathrm{ex}}\left(\rho(\mathbf{r})\right)+\frac{k_B T}{12}|\nabla\rho(\mathbf{r})|^2\int r^2 c_0^{(2)}(r)\mathrm{d}\mathbf{r}\right\} \tag{17}$$

where

$$c_0^{(2)}(|\mathbf{r}-\mathbf{r}'|)=-\left.\frac{\delta^2\beta F^{\mathrm{ex}}}{\delta\rho(\mathbf{r})\delta\rho(\mathbf{r}')}\right|_{\rho(\mathbf{r})=\rho_{\mathrm{b}}} \tag{18}$$

is the direct correlation function. Gradient approximation has been developed into the famous generalized gradient approximation (GGA) in quantum DFT but it is not so successful in CDFT. Although gradient approximation is more advanced than LDA, it is still invalid once the fluctuation of $\rho(\mathbf{r})$is strong. Besides, Eq. (17) is mathematically more complicated than Eq. (16), which makes the usage of gradient approximation even less than LDA.

### 2.2.3. Weighted density approximation (WDA)

WDA considers the guest-guest correlations by replacing the local density $\rho(\mathbf{r})$ in Eq. (16) with a weighted density [42, 43]:

$$\bar{\rho}(\mathbf{r})=\int \rho(\mathbf{r}')w(\mathbf{r}-\mathbf{r}')\mathrm{d}\mathbf{r}' \tag{19}$$

where $w(\mathbf{r})$ is the so-called weighting function. By applying the weighted density, the excess free energy is written by:

$$F_{\mathrm{WDA\text{-}V}}^{\mathrm{ex}}=\int f_{\mathrm{V}}^{\mathrm{ex}}(\bar{\rho}(\mathbf{r}))\mathrm{d}\mathbf{r} \tag{20}$$

or

$$F_{\mathrm{WDA\text{-}N}}^{\mathrm{ex}}=\int \rho(\mathbf{r})f_{\mathrm{N}}^{\mathrm{ex}}(\bar{\rho}(\mathbf{r}))\mathrm{d}\mathbf{r} \tag{21}$$

where $f_{\mathrm{N}}^{\mathrm{ex}}(\rho)$ is the excess free energy density (per molecule) as a function of fluid density for homogeneous systems, which can be obtained (along with $f_{\mathrm{V}}^{\mathrm{ex}}(\rho)$) by the corresponding equation of state (EOS). Compared to LDA and gradient approximation, WDA seems much more reliable according to its wide applications for both classical and quantum systems. The introduction of weighted density avoids the singular point of $f^{\mathrm{ex}}(\rho(\mathbf{r}))$ when $\rho(\mathbf{r}) \to \infty$ and can be used for systems with strong inhomogeneity, such as in MOF adsorption.

In WDA, there are different choices of the weighting function, which correspond to different versions of WDA. The simplest version of $w(\mathbf{r})$ is the Heaviside step function [42]:

$$w(\mathbf{r}) = \frac{3}{4\pi\sigma^3}\Theta(r-\sigma) \tag{22}$$

where

$$\Theta(x) = \begin{cases} 0 & x > 0 \\ 1 & x < 0 \end{cases} \tag{23}$$

and $\sigma$ is the molecular diameter. The advanced version is regarding the $w$ as a function of density profile, $w(\mathbf{r}-\mathbf{r}';\rho(\mathbf{r}))$, and solve $w(\mathbf{r}-\mathbf{r}';\rho(\mathbf{r}))$ from relevant closures. Typical examples are Curtin-Ashcroft's WDA [44]:

$$-\tilde{c}_0^{(2)}(k,\rho) = 2\frac{\mathrm{d}\beta f_{\mathrm{N}}^{\mathrm{ex}}(\rho)}{\mathrm{d}\rho}\tilde{w}(k,\rho) + \rho\frac{\partial}{\partial\rho}\left[\frac{\mathrm{d}\beta f_{\mathrm{N}}^{\mathrm{ex}}(\rho)}{\mathrm{d}\rho}\tilde{w}^2(k,\rho)\right] \tag{24}$$

where subscript "~" stands for the Fourier transform, Tarazona's WDA [45]:

$$w(r,\rho) = w_0(r) + w_1(r)\rho + w_1(r)\rho^2 + \cdots \tag{25}$$

modified WDA (MWDA) [46]

$$w(r,\rho) = -\frac{\mathrm{d}\rho}{2\mathrm{d}f_{\mathrm{N}}^{\mathrm{ex}}(\rho)}\left[k_{\mathrm{B}}Tc_0^{(2)}(r,\rho) + \frac{\rho}{V}\cdot\frac{\mathrm{d}^2 f_{\mathrm{N}}^{\mathrm{ex}}(\rho)}{\mathrm{d}\rho^2}\right] \tag{26}$$

Denton-Ashcroft's version [47]:

$$w(r,\rho) = c_0^{(2)}(r,\rho)\frac{\mathrm{d}\rho}{\mathrm{d}c_0^{(1)}(\rho)} \tag{27}$$

and hybrid WDA (HWDA) [48].

$$-\tilde{c}_0^{(2)}(k,\rho) = 2\frac{\mathrm{d}\beta f_{\mathrm{N}}^{\mathrm{ex}}(\rho)}{\mathrm{d}\rho}\tilde{w}(k,\rho) + \rho\frac{\mathrm{d}\beta f_{\mathrm{N}}^{\mathrm{ex}}(\rho)}{\mathrm{d}\rho}\tilde{w}^2(k,\rho) \tag{28}$$

The sophisticated WDA gives more accurate predictions on one hand but increases the computational cost on the other hand. It seems there is a trade-off between accuracy and computational cost. For MOF adsorption, the computational cost is an important factor and a simple weighting function like Eq. (22) may be more preferred.

### *2.2.4. Mean field approximation (MFA)*

According to statistical mechanics, the excess free energy can be exactly written by:

$$F^{\mathrm{ex}} = \frac{1}{2}\iint \rho(\mathbf{r})\rho(\mathbf{r}')g(\mathbf{r},\mathbf{r}')u(|\mathbf{r}-\mathbf{r}'|)\,\mathrm{d}\mathbf{r}\,\mathrm{d}\mathbf{r}' \tag{29}$$

where $g(\mathbf{r}, \mathbf{r}')$ is the radial distribution function (RDF) for inhomogeneous fluids, and $u(\mathbf{r}, \mathbf{r}')$ is the two-body interacting potential. Different from that of homogeneous system, the RDF for inhomogeneous fluids is a 6-dimensional function, which is difficult to obtain. The simplest approximation is to let

$$g(\mathbf{r},\mathbf{r}') = 1 \tag{30}$$

which leads to the so-called MFA:

$$F_{\mathrm{MFA}}^{\mathrm{ex}} = \frac{1}{2}\iint \rho(\mathbf{r})\rho(\mathbf{r}')u(|\mathbf{r}-\mathbf{r}'|)\,\mathrm{d}\mathbf{r}\,\mathrm{d}\mathbf{r}' \tag{31}$$

Although Eq. (30) seems to be a coarse approximation, MFA is still successful in various real applications. Due to its efficiency, MFA seems to be a potential method for MOF adsorption [49–51].

### *2.2.5. Functional expansion*

Functional expansion theory expands the excess free energy functional with respect to the bulk system as a Taylor series:

$$F^{\mathrm{ex}} = F_{\mathrm{b}}^{\mathrm{ex}} + \mu_{\mathrm{b}}^{\mathrm{ex}}\int \Delta\rho(\mathbf{r})\mathrm{d}\mathbf{r} - \frac{k_{\mathrm{B}}T}{2}\iint c_0^{(2)}(\mathbf{r}-\mathbf{r}')\Delta\rho(\mathbf{r})\Delta\rho(\mathbf{r}')\mathrm{d}\mathbf{r}\mathrm{d}\mathbf{r}' + \cdots \tag{32}$$

where $F_{\mathrm{b}}^{\mathrm{ex}}$ and $\mu_{\mathrm{b}}^{\mathrm{ex}}$ are the excess free energy and excess chemical potential for the bulk system, respectively; $\Delta\rho(\mathbf{r})=\rho(\mathbf{r})-\rho_{\mathrm{b}}$ is the deviation of density with respect to its bulk value. A common treatment of Eq. (32) is to truncate the series at the second order, which is the so-called square functional expansion (SFE). An intuitive understanding of SFE is that $\Delta\rho(\mathbf{r})$ should be small, otherwise the high-order terms should be considered. However, in real application, it seems the second-order truncation is valid even though $\Delta\rho(\mathbf{r})$ is so large [32, 52].

### *2.2.6. Fundamental measure theory (FMT)*

Different from the universal theories introduced above, FMT is specific for hard sphere fluids, where the interacting potential is given by:

$$u_{\mathrm{hs}}(r)=\begin{cases}\infty & r<\sigma\\ 0 & r>\sigma\end{cases} \tag{33}$$

where $\sigma$ is the hard sphere diameter. According to the decomposing of Heaviside function, FMT represents the excess free energy by [9, 13]:

$$\beta F^{\mathrm{ex}}=\int \Phi[n_{\alpha}(\mathbf{r})]\mathrm{d}\,\mathbf{r} \tag{34}$$

and

$$\Phi = f_0(n_3)n_0 + f_{12}(n_3)n_1n_2 + f_{222}(n_3)n_2^3 + f_{12}^{\mathrm{V}}(n_3)\mathbf{n}_{\mathrm{V1}}\cdot\mathbf{n}_{\mathrm{V2}} + f_{222}^{\mathrm{V}}(n_3)n_2(\mathbf{n}_{\mathrm{V2}}\cdot\mathbf{n}_{\mathrm{V2}}) \tag{35}$$

where $n_\alpha$ are weighted density:

$$n_{\alpha}(\mathbf{r})=\int \rho(\mathbf{r})\omega^{(\alpha)}(\mathbf{r}-\mathbf{r}')\mathrm{d}\mathbf{r}' \tag{36}$$

where

$$\begin{cases}\omega^{(3)}=\theta(|\mathbf{r}|-\sigma/2)\\ \omega^{(2)}(\mathbf{r})=\delta(r-\sigma/2)\\ \omega^{(1)}(\mathbf{r})=\dfrac{1}{2\pi\sigma}\delta(r-\sigma/2)\\ \boldsymbol{\omega}^{(\mathrm{V2})}(\mathbf{r})=\dfrac{\mathbf{r}}{r}\delta(|\mathbf{r}|-\sigma/2)\\ \boldsymbol{\omega}^{(\mathrm{V1})}(\mathbf{r})=\dfrac{\mathbf{r}}{2\pi\sigma r}\delta(|\mathbf{r}|-\sigma/2)\end{cases} \tag{37}$$

$f_i$ is undetermined coefficient, which can be determined by the bulk limit of Eq. (35). Applying the Carnahan-Starling (CS) equation of state, one can obtain Rosenfeld's original FMT:

$$\begin{cases} \Phi = \Phi_S + \Phi_V \\ \Phi_S = -n_0 \ln(1-n_3) + \dfrac{n_1 n_2}{1-n_3} + \dfrac{n_2^3}{24\pi(1-n_3)^2} \\ \Phi_V = -\dfrac{\mathbf{n}_{V1} \cdot \mathbf{n}_{V2}}{1-n_3} - \dfrac{n_2(\mathbf{n}_{V2} \cdot \mathbf{n}_{V2})}{8\pi(1-n_3)^2} \end{cases} \tag{38}$$

Applying the Boublik-Mansoori-Carnahan-Starling-Leland (BMCSL) equation of state, one can obtain Yu et al.'s modified FMT (MFMT) [17].

$$\begin{cases} \Phi = \Phi_S + \Phi_V \\ \Phi_S = -n_0 \ln(1-n_3) + \dfrac{n_1 n_2}{1-n_3} + \left[\dfrac{\ln(1-n_3)}{36\pi n_3^2} + \dfrac{1}{36\pi n_3(1-n_3)^2}\right] n_2^3 \\ \Phi_V = -\dfrac{\mathbf{n}_{V1} \cdot \mathbf{n}_{V2}}{1-n_3} - \left[\dfrac{\ln(1-n_3)}{12\pi n_3^2} + \dfrac{1}{12\pi n_3(1-n_3)^2}\right] n_2(\mathbf{n}_{V2} \cdot \mathbf{n}_{V2}) \end{cases} \tag{39}$$

FMT excellently captures the properties for hard sphere system with low computational costs and is the most favorable theory for hard sphere fluids in CDFT [19, 28, 35, 53].

### *2.2.7. Hybrid method*

In real application, it is more common to apply two or more approximations for one system. Generally, molecule-molecule interactions can be decoupled into different contributions such as repulsive interactions, attractive interactions, and electrostatic interactions, which have different effects on fluids' properties. In this case, to separate the excess free energy into different terms corresponding to the different interactions and applying different approximations for each term seems more efficient than a single approximation.

For spherical molecules such as $CH_4$, $H_2$, and $N_2$, the excess free energy is usually separated into the hard sphere contribution $F^{hs}$, representing the repulsive interaction and the attractive contribution $F^{attr}$:

$$F^{ex} = F^{hs} + F^{attr} \tag{40}$$

By applying different approximations to $F^{hs}$ and $F^{attr}$, respectively, one can formulate the complete expression of excess free energy. For example, see [25, 54], Yu et al. have employed

MFMT and WDA to approximate $F^{\mathrm{hs}}$ and $F^{\mathrm{attr}}$, respectively, and predicted the gas adsorption and phase transition in MCM-41; Ritter et al. [55] have employed FMT and MFA to study the binary gas adsorption in heterogeneous BPL-activated carbon; Siderius et al. [27] have applied WDA and MFA to predict $H_2$ adsorption in MOF-5, which has then been improved by two versions of WDA in Liu et al.'s work [26]. Recently, Yu et al. [28] have introduced a correlation term $F^{\mathrm{cor}}$ to Eq. (40):

$$F^{\mathrm{ex}} = F^{\mathrm{hs}} + F^{\mathrm{attr}} + F^{\mathrm{cor}} \tag{41}$$

which has soon been applied to MOF adsorptions by Liu and Wu et al. [31, 33–35].

## 3. Applying CDFT to MOF adsorption

Although the framework of CDFT has been established for a long time, its application to MOF adsorption had not been reported until 2009. **Table 1** lists current reports of applying CDFT on MOF adsorption. There is an obvious transition of these reports from 2010 to 2013, where the time cost decreases from 10 days to less than 1 minute. As will be introduced later, this is the benefit of acceleration method. Later in this section, we will introduce the typical studies listed in this table.

| Year | System | | Method | Time cost per calculation | Ref. |
|---|---|---|---|---|---|
| | Adsorbate | Adsorbent | | | |
| 2009 | $H_2$ | MOF-5 | WDA + MFA | | [27] |
| 2009 | $H_2$ | MOF-5, ZIF-8 | WDA + WDA | 5 days | [26] |
| 2010 | $CO_2/CH_4$, $CO_2/N_2$ | ZIF-8, $Zn_2(BDC)_2(ted)$ | WDA + WDA | 10 days | [29] |
| 2013 | $H_2$, He, Ne, Ar | MOF-5, MFI, CuBTC, ZIF-8 | MFMT + MFA +WDA | <1 min. | [31] |
| 2015 | $H_2$ | 1200 MOFs | 5 versions | 20 s | [33] |
| 2015 | $CH_4$ | 1200 MOFs | 4 versions | 2 min. | [36] |
| 2015 | $H_2$ | 712 MOFs × 21 temperatures × 21 pressures | MFMT + MFA +WDA | 18 s | [35] |
| 2015 | DBT | 458 MOFs | MFMT + MFA +WDA | 20 s | [34] |

**Table 1.** Applications of CDFT on MOF adsorption.

### 3.1. Initial application

The first report of the application is done by Siderius et al. [27]. Siderius et al. have employed Tarazona's WDA and MFA to construct the hard sphere and attractive free energy functional, and applied the theory to $H_2$ adsorption in MOF-5 (**Figure 1(a)**). Siderius et al.'s CDFT predictions accord with simulations and experiments very well at room temperature, but lower the estimated uptake in low temperature region (**Figure 1**).

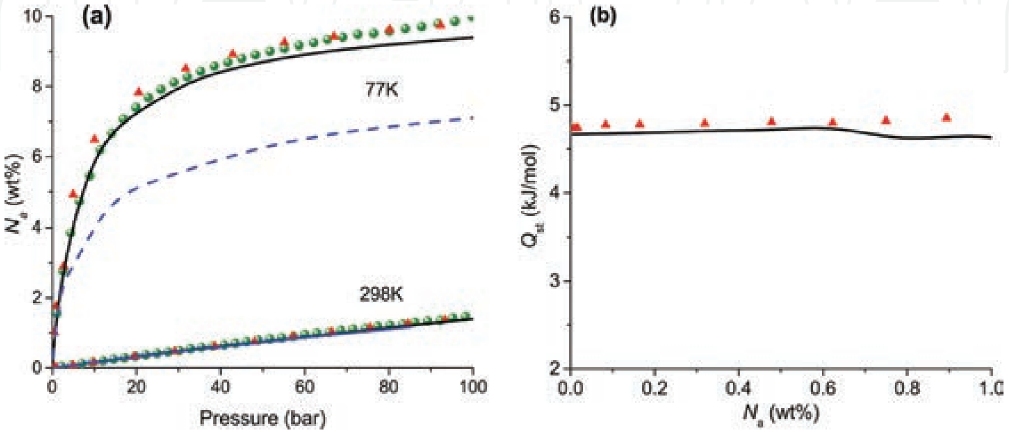

**Figure 1.** CDFT prediction of $H_2$ adsorption in MOF-5, (a) uptake, (b) isosteric heat. Solid line: Liu et al.'s CDFT; dashed line: Siderius et al.'s CDFT; triangle: MC simulation; sphere: experiments. Reprinted with permission from Ref. [26]. Copyright (2016) American Chemical Society.

Such shortcomings were soon solved by Liu et al. [26]. Liu et al. have employed two versions of WDA to approximate the hard sphere and attractive free energy, respectively. Liu et al.'s CDFT well predicted the adsorption isotherm and the isosteric heat for both high and low temperatures. Siderius et al. and Liu et al.'s CDFT have also revealed the microscopic conformation of the adsorbed gases. As shown in **Figure 2**, at low pressure, $H_2$ is mainly distributed at the favorable adsorption site, while at high pressure, $H_2$ is distributed at both the favorable adsorption sites and the surface of framework. These are consistent with other simulation findings.

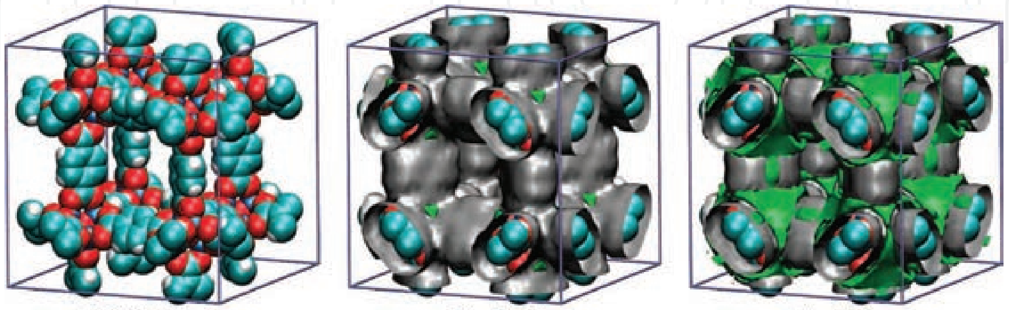

A) IRMOF-1 Structure B) p=79.5 bar C) p=179 bar

**Figure 2.** Molecular structure of MOF-5 (IRMOF-1) and density isosurface of $H_2$ in MOF-5 at 298 K. Color of the isosurface: gray, 1.33 mol/L; green, 19.9 mol/L. Color of the atoms: dark blue, Zn; light blue, C; red, O; white, H [27]. Reprinted with permission from Ref. [27]. Copyright (2016) American Chemical Society.

The theory has then been extended to mixtures by Liu et al. in 2010 [29]. Similar to that for pure component, two versions of WDA have been employed to construct the excess free energy functional, where the BMCSL and the modified Benedicit-Webb-Rubin (MBWR) equation of state have been used to formulate the free energy density which is required in WDA. Liu et al. considered $CO_2/CH_4$ and $CO_2/N_2$ separation in two types of MOFs, respectively, where CDFT accords with simulations very well (**Table 2**).

| | ZIF-8 | $Zn_2(BDC)_2(ted)$ |
|---|---|---|
| $CO_2/CH_4$ (1:1) | 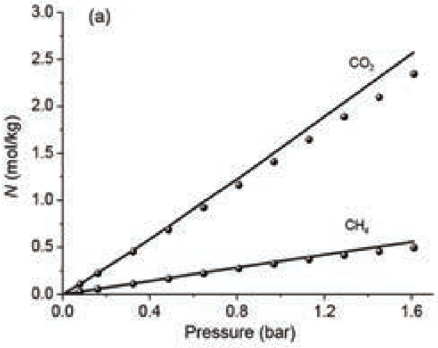 | 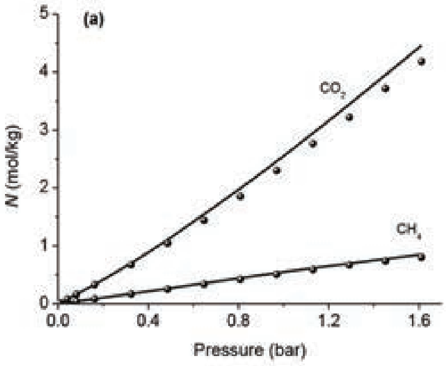 |
| $CO_2/N_2$ (15:85) | 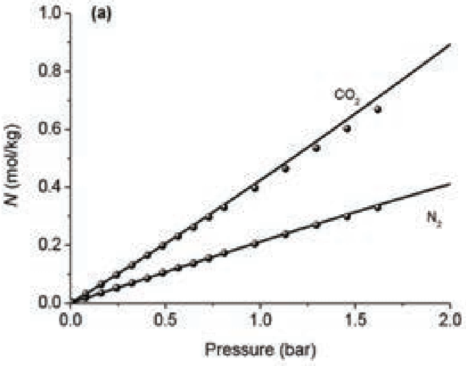 | 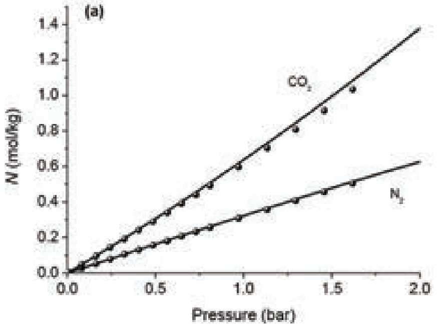 |

*Line: CDFT prediction; dot: MC simulation.
Adapted with permission from Ref. [29]. Copyright (2016) American Chemical Society.

**Table 2.** Adsorption isotherm for $CO_2/CH_4$ and $CO_2/N_2$ in two MOFs*.

### 3.2. Acceleration method

Siderius et al. and Liu et al.'s work have demonstrated that CDFT can be used to predict gas adsorption in MOFs, however, there is a fatal flaw in these initial studies: the computational cost is too high. Before the application to MOF adsorption, CDFT mainly focuses on simple geometric systems such as slit pores and cylindrical pores, where the computation is very efficient. However, when applying to 3-dimensional structured systems such as MOFs, the computational cost is unacceptable if an ordinary numerical treatment is employed. In principle, the accuracy of CDFT cannot exceed simulations; once the computational cost of CDFT is higher than simulation, CDFT will be useless in an application view.

Fortunately, CDFT can be accelerated. The most time consuming part of CDFT is the 3-dimensional integration such as Eqs. (19) and (36). These integrations can be simplified into 1-dimensional integration for slit and cylindrical pores but not for MOFs. However, as most of these integration are convolutions, which takes the form of:

$$A(\mathbf{r}) = \int B(\mathbf{r}')C(\mathbf{r}-\mathbf{r}')\,\mathrm{d}\mathbf{r}' \tag{42}$$

By using the Fourier transform on both sides of Eq. (42), the convolution can be transformed into:

$$A = \mathcal{F}^{-1}\left[\mathcal{F}\left(B\right)\cdot\mathcal{F}\left(C\right)\right] \tag{43}$$

where $\mathcal{F}$ and $\mathcal{F}^{-1}$ stand for the forward and backward Fourier transform, respectively. By applying the fast Fourier transform (FFT) algorithm, the complexity of Eq. (43) is in order of $n\log_2 n$, where $n$ is the number of the discrete sites of the system. In contrast, the complexity of Eq. (42) is in order of $n^2$. For MOF adsorption, a typical value of $n$ is $50^3 = 125{,}000$, which means applying Eq. (43) will accelerate the computation by more than 5 orders of magnitude. By applying FFT, the typical time cost for MOF adsorption is about 10–20 seconds, which is faster than state-of-the-art simulations by orders of magnitudes.

The introduction of FFT is a revolutionary advance in 3D-CDFT and makes 3D-CDFT much faster than simulations. With FFT, CDFT becomes a competitive method in predicting MOF adsorptions.

### 3.3. High-throughput calculation

One of the significant applications of the accelerated CDFT is material screening. Due to the various metal clusters, organic linkers, and 3-dimensional structures, there are billions of MOFs in principle. How to identify the best MOF in such a large database is an essential issue in material design. The traditional method to do this is the molecular simulation. Snurr et al. [1] have performed MC simulation of methane adsorption in 137,953 hypothetical MOFs and have screened out 300 MOFs which have higher methane capacity than any real MOFs. Based on the screening, Snurr et al. have synthesized a high-performance methane storage material, NOTT-107. Snurr et al.'s work has demonstrated the feasibility of high-throughput screening. However, Snurr et al.'s MC simulation is computationally expensive, which may not be the best method for high-throughput calculation. As mentioned above, as the accelerated CDFT is faster than MC simulation by two orders of magnitudes, CDFT seems to be a better choice.

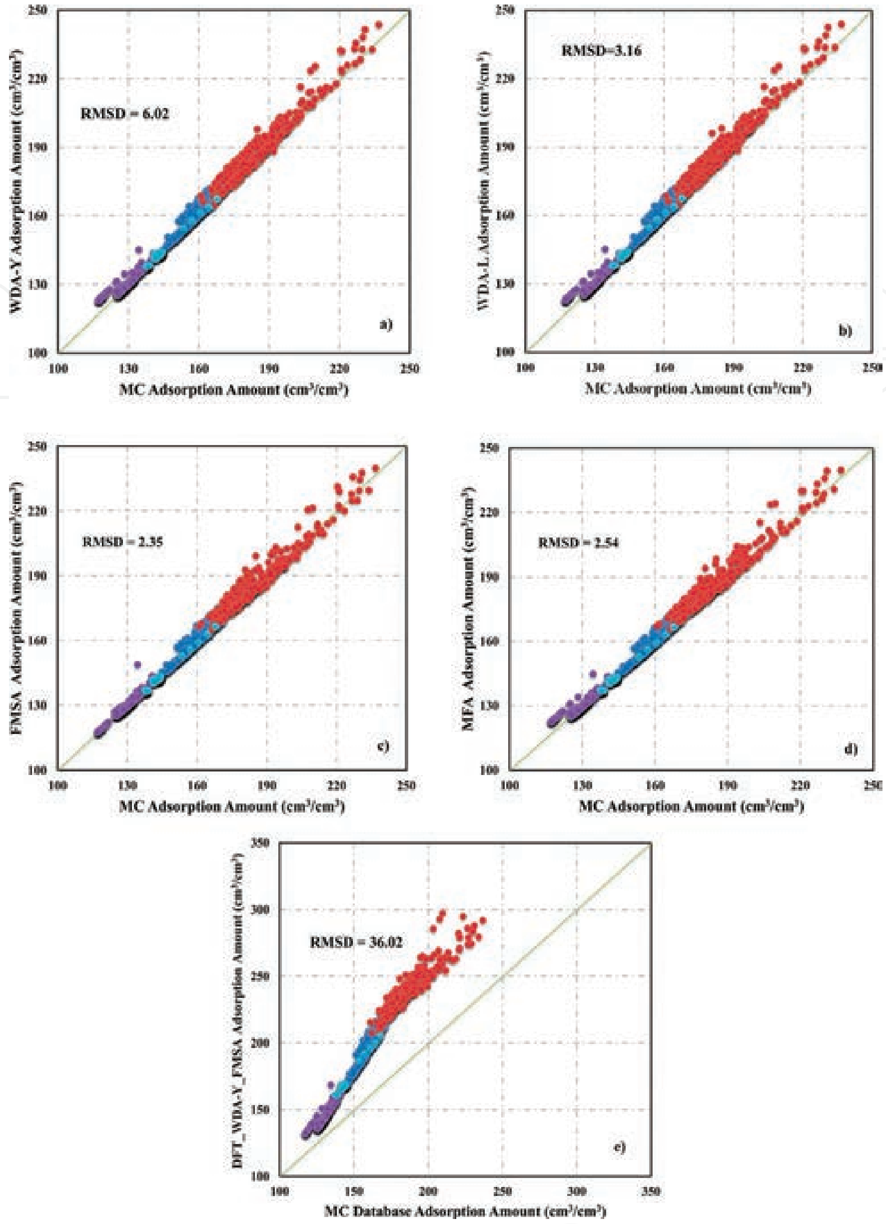

**Figure 3.** Uptake of $H_2$ in 1200 MOF at 243 K, 100 bar, comparison between five versions of CDFT and MC simulation. The versions for CDFT are (a) MFMT + WDA-V(MBWR) + MFA; (b) MFMT + WDA-N(MBWR) + MFA; (c) MFMT + SFE; (d) MFMT + MFA; (e) MFMT + WDA-V(FMSA) + MFA [33]. Reprinted with permission from Ref. [33]. Copyright (2016) American Chemical Society.

Applying CDFT to high-throughput screening has been reported very recently by Liu and Wu et al. [33–36]. First, Liu and Wu et al. [33] have predicted $H_2$ adsorption in 1200 MOFs by CDFT. As shown in **Figure 3**, five versions of CDFT have been tested. In **Figure 3(a),(b)**, and **(e)**, the excess free energy is given by Eq. (41), where $F^{\text{hs}}$, $F^{\text{attr}}$, and $F^{\text{cor}}$ are approximated by MFMT, MFA, and WDA, respectively; the "MBWR" and "FMSA" in the brackets mean the correlation free energy density used in WDA that is calculated by MBWR EOS and FMSA (first-order mean sphere approximation) EOS [56], respectively. In **Figure 3(c)** and **(d)**, the excess free energy is represented by Eq. (40), where $F^{\text{hs}}$ is approximated by MFMT for both, while $F^{\text{attr}}$ is approximated by SFE and MFA, respectively. It seems the first four versions of CDFT accord with simulations very well in contrast to the last one, where the correlation free energy density is approximated by FMSA. This reveals that the accuracy of EOS plays an important role in the accuracy of WDA, and the MBWR seems a good choice for MOF adsorption. To give a more comprehensive judgment of the other four versions of CDFT, Liu and Wu et al. have compared CDFT and simulation on different conditions. **Table 3** shows the root-mean-square deviation (RMSD) of the four CDFTs with respect to MC simulations. It seems MFMT + WDA-V + MFA and MFMT + WDA-N + MFA are the two most stable versions, while MFMT + SFE and MFMT + MFA are not so accurate at low temperatures. Besides, Liu and Wu et al.'s CDFT is processed in a single core (Intel E1230) with time cost around 10–20 seconds for each calculation, which is much faster than simulations (**Figure 4**).

| | **243 K 100 bar** | **77 K 1 bar** | **77 K 50 bar** |
|---|---|---|---|
| **MFMT + WDA-V + MFA** | 6.02 | 6.87 | 17.2 |
| **MFMT + WDA-N + MFA** | 3.16 | 8.38 | 16.9 |
| **MFMT + SFE** | 2.35 | 27 | 40.3 |
| **MFMT + MFA** | 2.54 | 11.3 | 39.3 |

**Table 3.** The RMSD of CDFT in different conditions (unit: $cm^3$ (STP) /$cm^3$).

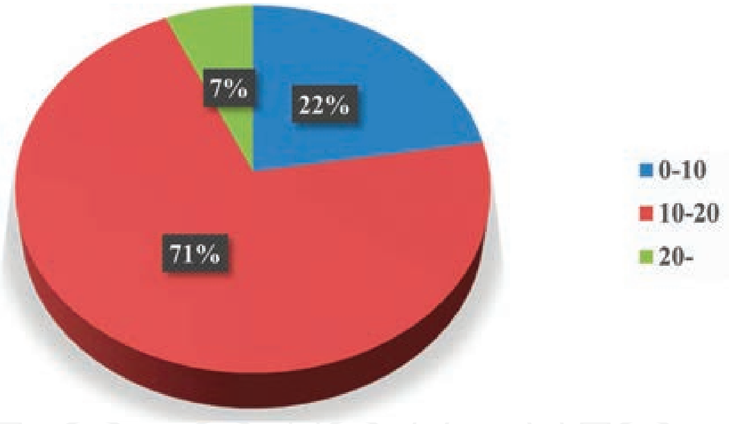

**Figure 4.** Time cost of the CDFT calculation for $H_2$ adsorption in 1200 MOFs (unit: second). Reprinted with permission from Ref. [33]. Copyright (2016) American Chemical Society.

CDFT has then been applied to screen out hydrogen storage materials for different conditions. By using CDFT, Liu et al. [35] have predicted $H_2$ adsorption in 712 MOFs under 441 different conditions. The whole computation (712 × 441 = 313,992 cases in total) only takes approximately 1500 CPU hours.

As shown in **Figure 5**, Liu et al. have predicted the highest uptake of the 712 MOFs at temperature 77–373 K, pressure 0.01–100 atm. On one hand, the uptake of the MOFs at low temperature is striking: At 77 K 100 atm, the highest uptake is approximately 37 mol/L, exceeding the density of liquid hydrogen; even at low pressure, 77 K 0.01 atm, the highest uptake approaches 13 mol/L, which is higher than many real MOFs at high pressures. On the

http://dx.doi.org/10.5772/64632

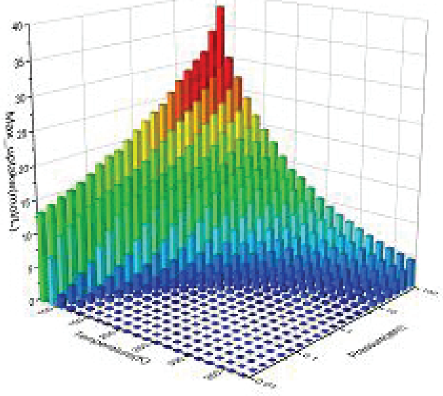

**Figure 5.** The highest uptakes of 712 types of MOF materials at different temperature and pressure [35]. Reprinted with permission from Ref. [35]. Copyright (2016) John Wiley & Sons, Inc.

other hand, the uptake at high temperature is not so satisfactory; most uptakes are lower than 5 mol/L. It appears that hydrogen storage at high temperature is still a big problem which is difficult to be solved by MOFs.

Based on Liu et al.'s screening, a set of promising MOFs have been identified. **Figure 6** shows the three promising MOFs and their adsorption isotherm for hydrogen storage at high, medium and low loadings, respectively. It seems narrower pore is more preferred for high temperatures in contrast to low temperatures.

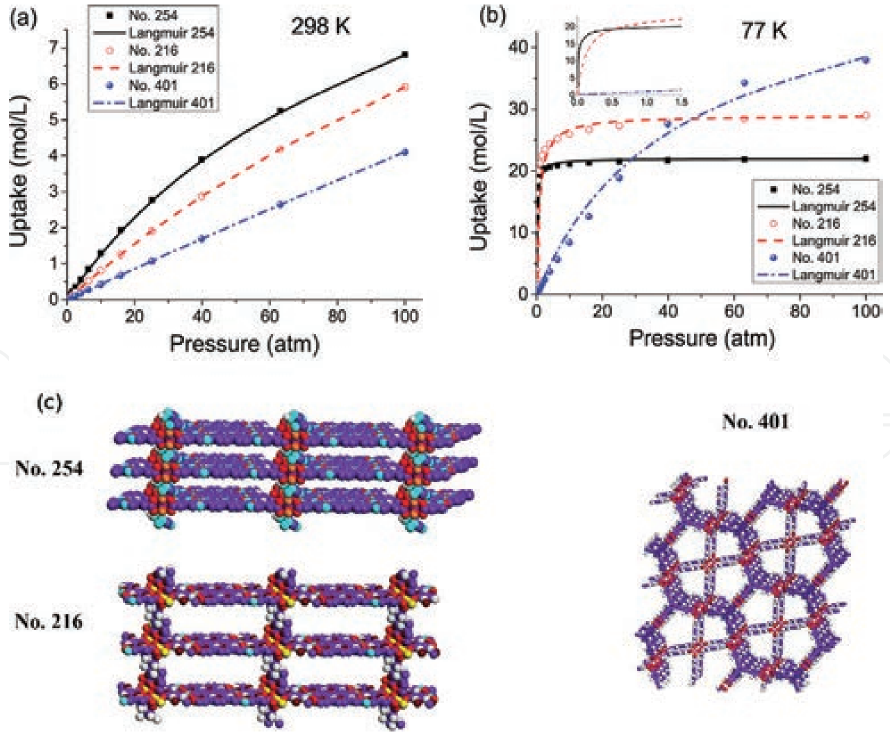

**Figure 6.** Adsorption isotherms for three MOF structures at (a) 298 K; (b) 77 K. (c) Structure of the three MOFs, color codes: C, purple; H, white; O, red; N, light blue; Zn: pink; Cu: orange; Br: wine; V: yellow [35]. Reprinted with permission from Ref. [35]. Copyright (2016) John Wiley & Sons, Inc.

Besides hydrogen storage, CDFT has also been extended to other screenings such as methane storage [36] and desulfurization [34]. Again, CDFT has revealed itself as a more efficient method than simulations in these high-throughput calculations.

### 3.4. Entropy scaling

Besides the density profile and uptake, CDFT could also predict other important properties of MOF adsorption, such as entropy and even self-diffusivity.

To generate entropy from CDFT is straightforward as the free energy functional is given explicitly in CDFT. Entropy can be obtained by a simple derivative:

$$S = -\left(\frac{\partial F}{\partial T}\right)_{\rho(\mathbf{r})} \tag{44}$$

One of the most important usage of entropy is the entropy scaling rule, which was proposed by Rosenfeld in 1977 [57] and explained by Dzugutov in 1996 [58]. The entropy scaling rule correlates excess entropy and self-diffusivity by a universal equation:

$$D^* = A\exp(Bs^{\mathrm{ex}^*}) \tag{45}$$

where $D^*$ is the dimensionless self-diffusivity, $s^{\mathrm{ex}^*}$ is the dimensionless excess entropy, $A$ and $B$ are universal constants that are independent of external conditions and molecular models. Eq. (45) had been first introduced for homogeneous fluids; however, Truskett et al. [59–61] have shown that the correlations between entropy and diffusivity also exist in inhomogeneous fluids. Recently, Liu et al. [31] have applied entropy scaling rule together with CDFT, MD simulation, and mean free volume theory to predict the self-diffusivity of MOFs:

$$\ln D_{\mathrm{s}} = \left(1 - \frac{\alpha N \sigma^3}{V_{\mathrm{free}}}\right)\ln D_{\mathrm{K}} + \frac{\alpha N \sigma^3}{V_{\mathrm{free}}}\ln D_{\mathrm{E}} \tag{46}$$

where $D_{\mathrm{s}}$ is the self-diffusivity of fluids in MOFs, $D_{\mathrm{K}}$ is the Knudsen diffusivity, which can be calculated by one MD simulation, $D_{\mathrm{E}}$ is the diffusivity calculated from entropy scaling rule and CDFT, i.e., Eq. (45), $V_{\mathrm{free}}$ is the free volume and $\alpha$ is the mixing parameter, which can be determined from face center cubic (FCC) approximation or empirical method. Liu et al. have applied Eq. (46) to predict the self-diffusivity of fluids in MOFs. **Figure 7** shows the comparison between Eq. (46) and pure MD simulations. It seems combining CDFT and entropy scaling rule could capture the essentials of the diffusion curve, and Eq. (46) may accelerate the prediction of self-diffusivities.

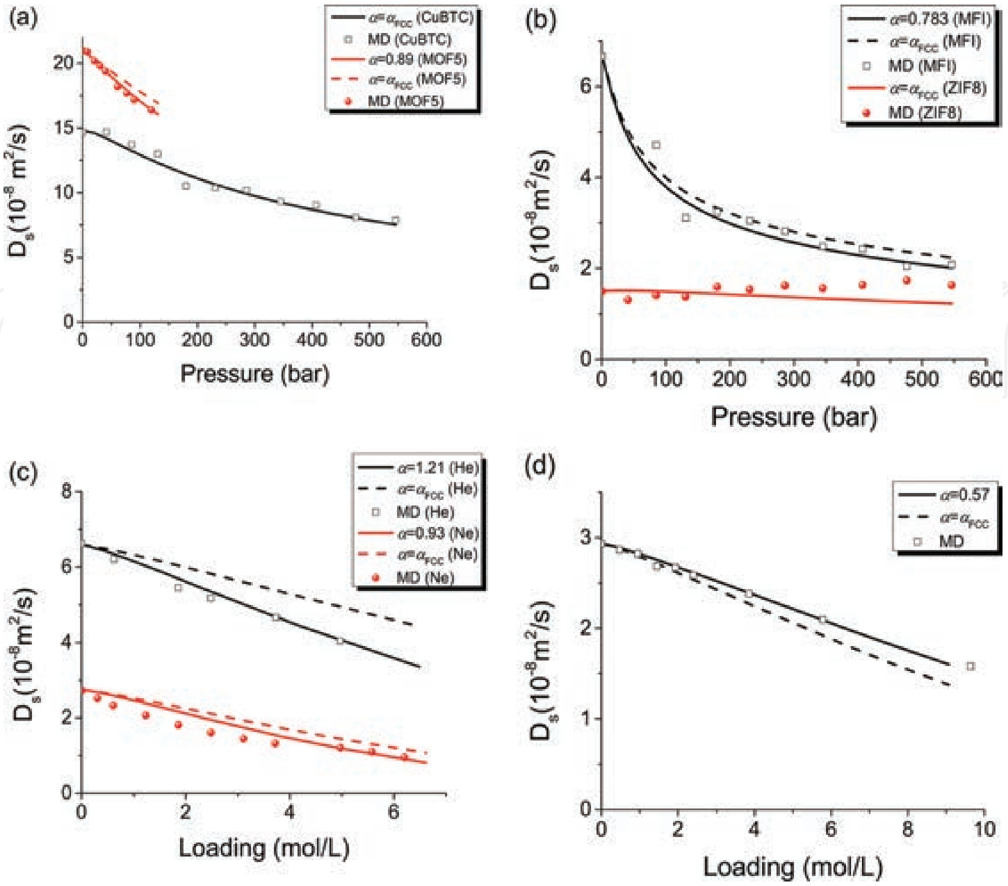

**Figure 7.** Self-diffusivity of (a) $H_2$ in CuBTC and MOF-5; (b) $H_2$ in MFI and ZIF-8; (c) He and Ne in MFI; (d) Ar in MOF-5. Comparison between CDFT-based entropy scaling rule and MD simulation [31]. Reprinted with permission from Ref. [31]. Copyright (2016) American Chemical Society.

## 4. Conclusion and prospect

We have introduced the theoretical framework of CDFT and reviewed the applications of using CDFT to predict fluid adsorption in MOFs. Although the framework of CDFT had been proposed 40 years ago, its application on real system such as MOF adsorption is still a new frontier. The applications of CDFT on MOF adsorption are reported in the past 6–7 years and mainly come from a few research groups. However, CDFT has been successfully applied to gas adsorption/diffusion in nanoporous materials and high-throughput screening of MOFs. In these applications, the FFT seems to be the key which makes CDFT more efficient than conventional simulations. One reason for the relatively fewer applications of CDFT is the lack of CDFT software in the current stage. Developing a usable CDFT software would extend the application of CDFT.

Besides the advantages, the challenge of current CDFT is how to deal with polar molecules which may not be coarse grained into a spherical model such as $H_2O$. It is well known that the hydrogen bonding network instead of spherical Van der Waals interaction is the dominating factor of such polar systems. For non-spherical molecule, the difficulty is how to construct an accurate excess free energy functional which can be accelerated by numerical method such as Eq. (43). For example, in MFA, Eq. (31), the molecule-molecule interaction $u(\mathbf{R}_1, \mathbf{R}_2)$is a multi-dimensional function which cannot be simplified into a one-dimensional function $u(r)$; in functional expansion theory, the high-order terms (so-called bridge functional) give an important contribution, which often cannot be accelerated by FFT. If such problems are solved, CDFT will be a perfect substitute for MC simulation.

## Acknowledgements

This work is sponsored by the National Natural Science Foundation of China (No. 21506051, 91334203), the 111 Project of Ministry of Education of China (No. B08021), the Shanghai Pujiang Program (15PJ1401400), the Open Project of State Key Laboratory of Chemical Engineering (SKL-Che-15C05), and the Fundamental Research Funds for the Central Universities of China (222201414008).

## Author details

Yu Liu* and Honglai Liu

*Address all correspondence to: hlliu@ecust.edu.cn

State Key Laboratory of Chemical Engineering, Department of Chemical Engineering, East China University of Science and Technology, Shanghai, China

## References

[1] Wilmer CE, Leaf M, Lee CY, et al. Large-scale screening of hypothetical metal-organic frameworks. *Nature Chemistry*. 2012;4(2):83–89. DOI: 10.1038/nchem.1192

[2] Colon YJ, Snurr RQ. High-throughput computational screening of metal-organic frameworks. *Chemical Society Reviews*. 2014;43(16):5735–5749. DOI: 10.1039/c4cs00070f

[3] Wu D, Wang C, Liu B, Liu D, Yang Q, Zhong C. Large-scale computational screening of metal-organic frameworks for $CH_4/H_2$ separation. *Aiche Journal*. 2012;58(7):2078–2084. DOI: 10.1002/aic.12744

[4] Ebner C, Saam WF, Stroud D. Density-functional theory of simple classical fluids. I. Surfaces. *Physical Review A (General Physics)*. 1976;14(6):2264–2273. DOI: 10.1103/PhysRevA.14.2264

[5] Ebner C, Punyanitya C. Density-functional theory of simple classical fluids. II. Localized excess electron states. *Physical Review A (General Physics)*. 1979;19(2):856–865. DOI: 10.1103/PhysRevA.19.856

[6] Lado F, Foiles SM, Ashcroft NW. Solutions of the reference hypernetted-chain equation with minimized free-energy. *Physical Review A*. 1983;28(4):2374–2379. DOI: 10.1103/PhysRevA.28.2374

[7] Chandler D, McCoy JD, Singer SJ. Density functional theory of nonuniform polyatomic systems. 1. General formulation. *Journal of Chemical Physics*. 1986;85(10):5971–5976. DOI: 10.1063/1.451510

[8] Hansen JP, McDonald IR. *Theory of Simple Liquids*. 2nd Ed. London: Academic Press; 1986.

[9] Rosenfeld Y. Free-energy model for the inhomogeneous hard-sphere fluid mixture and density-functional theory of freezing. *Physical Review Letters*. 1989;63(9):980–983. DOI: 10.1103/physrevlett.63.980

[10] McMullen WE, Freed KF. A density functional theory of polymer phase transitions and interfaces. *The Journal of Chemical Physics*. 1990;92(2):1413–1426. DOI: 10.1063/1.458153

[11] Kierlik E, Rosinberg ML. Density-functional theory for inhomogeneous fluids: adsorption of binary-mixtures. *Physical Review A*. 1991;44(8):5025–5037. DOI: 10.1103/PhysRevA.44.5025

[12] Rosenfeld Y. Free-energy model for inhomogeneous fluid mixtures: Yukawa-charged hard-spheres, general interactions, and plasmas. *Journal of Chemical Physics*. 1993;98(10):8126–8148. DOI: 10.1063/1.464569

[13] Rosenfeld Y. Phase separation of asymmetric binary hard-sphere fluids: self-consistent density functional theory. *Physical Review Letters*. 1994;72(24):3831–3834. DOI: 10.1103/PhysRevLett.72.3831

[14] Perez-Jorda JM, Becke AD. A density-functional study of van der Waals forces: rare gas diatomics. *Chemical Physics Letters*. 1995;233(1–2):134–137. DOI: 10.1016/0009-2614(94)01402-h

[15] Seok C, Oxtoby DW. Nucleation in n-alkanes: a density-functional approach. *Journal of Chemical Physics*. 1998;109(18):7982–7990. DOI: 10.1063/1.477445

[16] Marconi UMB, Tarazona P. Dynamic density functional theory of fluids. *Journal of Chemical Physics*. 1999;110(16):8032–8044. DOI: 10.1063/1.478705

[17] Yu YX, Wu JZ. Structures of hard-sphere fluids from a modified fundamental-measure theory. *Journal of Chemical Physics*. 2002;117(22):10156–10164. DOI: 10.1063/1.1520530

[18] Yu YX, Wu JZ. A fundamental-measure theory for inhomogeneous associating fluids. *Journal of Chemical Physics*. 2002;116(16):7094–7103. DOI: 10.1063/1.1463435

[19] Yu YX, Wu JZ. Density functional theory for inhomogeneous mixtures of polymeric fluids. *Journal of Chemical Physics*. 2002;117(5):2368–2376. DOI: 10.1063/1.1491240

[20] Cao D, Wu J. Density functional theory for semiflexible and cyclic polyatomic fluids. *Journal of Chemical Physics*. 2004;121(9):4210–4220. DOI: 10.1063/1.1774983

[21] Li Z, Wu J. Density-functional theory for the structures and thermodynamic properties of highly asymmetric electrolyte and neutral component mixtures. *Physical Review E*. 2004;70(3 Pt 1):031109.

[22] Ye ZC, Cai J, Liu HL, Hu Y. Density and chain conformation profiles of square-well chains confined in a slit by density-functional theory. *Journal of Chemical Physics*. 2005;123(19):194902. DOI: 10.1063/1.2117009

[23] Ye Z, Chen H, Cai J, Liu H, Hu Y. Density functional theory of homopolymer mixtures confined in a slit. *Journal of Chemical Physics*. 2006;125(12):124705. DOI: 10.1063/1.2354087

[24] Yu YX, You FQ, Tang YP, Gao GH, Li YG. Structure and adsorption of a hard-core multi-Yukawa fluid confined in a slitlike pore: grand canonical Monte Carlo simulation and density functional study. *Journal of Physical Chemistry B*. 2006;110(1):334–341. DOI: 10.1021/jp055299s

[25] Peng B, Yu Y-X. A density functional theory for Lennard-Jones fluids in cylindrical pores and its applications to adsorption of nitrogen on MCM-41 Materials. *Langmuir*. 2008;24(21):12431–12439. DOI: 10.1021/la8024099

[26] Liu Y, Liu HL, Hu Y, Jiang JW. Development of a density functional theory in three-dimensional nanoconfined space: $H_2$ storage in metal organic frameworks. *Journal of Physical Chemistry B*. 2009;113(36):12326–12331. DOI: 10.1021/jp904872f

[27] Siderius DW, Gelb LD. Predicting gas adsorption in complex microporous and mesoporous materials using a new density functional theory of finely discretized lattice fluids. *Langmuir*. 2009;25(3):1296–1299. DOI: 10.1021/la803666t

[28] Yu YX. A novel weighted density functional theory for adsorption, fluid-solid interfacial tension, and disjoining properties of simple liquid films on planar solid surfaces. *Journal of Chemical Physics*. 2009;131(2): 024704. DOI: 10.1063/1.3174928

[29] Liu Y, Liu HL, Hu Y, Jiang JW. Density functional theory for adsorption of gas mixtures in metal-organic frameworks. *Journal of Physical Chemistry B*. 2010;114(8):2820–2827. DOI: 10.1021/jp9104932

[30] Zhao S, Ramirez R, Vuilleumier R, Borgis D. Molecular density functional theory of solvation: from polar solvents to water. *Journal of Chemical Physics*. 2011;134(19):194102. DOI: 19410210.1063/1.3589142

[31] Liu Y, Fu J, Wu J. Excess-entropy scaling for gas diffusivity in nanoporous materials. *Langmuir*. 2013;29(42):12997–13002. DOI: 10.1021/la403082q

[32] Liu Y, Zhao S, Wu J. A site density functional theory for water: application to solvation of amino acid side chains. *Journal of Chemical Theory and Computation*. 2013;9(4):1896–1908. DOI: 10.1021/ct3010936

[33] Fu J, Liu Y, Tian Y, Wu J. Density functional methods for fast screening of metal-organic frameworks for hydrogen storage. *The Journal of Physical Chemistry C*. 2015;119:5374–5385. DOI: 10.1021/jp505963m

[34] Liu Y, Guo F, Hu J, Zhao S, Liu H, Hu Y. Screening of desulfurization adsorbent in metal-organic frameworks: a classical density functional approach. *Chemical Engineering Science*. 2015;137:170–177. DOI: 10.1016/j.ces.2015.06.036

[35] Liu Y, Zhao S, Liu H, Hu Y. High-throughput and comprehensive prediction of $H_2$ adsorption in metal-organic frameworks under various conditions. *AIChE Journal*. 2015;61:2951–2957. DOI: 10.1002/aic.14842

[36] Fu J, Tian Y, Wu J. Classical density functional theory for methane adsorption in metal-organic framework materials. *Aiche Journal*. 2015;61(9):3012–3021. DOI: 10.1002/aic.14877

[37] Rappe AK, Casewit CJ, Colwell KS, Goddard WA, Skiff WM. UFF, a full periodic table force field for molecular mechanics and molecular dynamics simulations. *Journal of the American Chemical Society*. 1992;114(25):10024–10035. DOI: 10.1021/ja00051a040

[38] Mayo SL, Olafson BD, Goddard WA, III. DREIDING: a generic force field for molecular simulations. *Journal of Physical Chemistry*. 1990;94(26):8897–8909. DOI: 10.1021/j100389a010

[39] Hohenberg P, Kohn W. Inhomogeneous electron gas. *Physical Review B*. 1964;136(3B):B864. DOI: 10.1103/PhysRev.136.B864

[40] Kohn W, Sham LJ. Self-consistent equations including exchange and correlation effects. *Physical Review*. 1965;140(4A):A1133–A1138. DOI: 10.1103/physrev.140.a1133

[41] Liu J, Herbert JM. Local excitation approximations to time-dependent density functional theory for excitation energies in solution. *Journal of Chemical Theory And Computation*. 2016;12(1):157–166. DOI: 10.1021/acs.jctc.5b00828

[42] Johnson M, Nordholm S. Generalized van der Waals theory. VI. Application to adsorption. *Journal of Chemical Physics*. 1981;75(4):1953–1957. DOI: 10.1063/1.442220

[43] Tarazona P, Evans R. A simple density functional theory for inhomogeneous liquids: wetting by gas at a solid-liquid interface. *Molecular Physics*. 1984;52(4):847–857. DOI: 10.1080/00268978400101601

[44] Curtin WA, Ashcroft NW. Weighted-density-functional theory of inhomogeneous liquids and the freezing transition. *Physical Review A (General Physics)*. 1985;32(5):2909–2919. DOI: 10.1103/PhysRevA.32.2909

[45] Tarazona P. Free energy density functional for hard spheres. *Physical Review A (General Physics)*. 1985;31(4):2672–2679. DOI: 10.1103/PhysRevA.31.2672

[46] Denton AR, Ashcroft NW. Modified weighted-density-functional theory of nonuniform classical liquids. *Physical Review A (General Physics)*. 11989;39(9):4701–4708. DOI: 10.1103/PhysRevA.39.4701

[47] Denton AR, Ashcroft NW. Density-functional approach to the structure of classical uniform fluids. *Physical Review A (Statistical Physics, Plasmas, Fluids, and Related Interdisciplinary Topics)*. 1991;44(2):1219–1227. DOI: 10.1103/PhysRevA.44.1219

[48] Leidl R, Wagner H. Hybrid WDA: a weighted-density approximation for inhomogeneous fluids. *Journal of Chemical Physics*. 1993;98(5):4142–4148. DOI: 10.1063/1.465022

[49] Ravikovitch PI, Vishnyakov A, Neimark AV. Density functional theories and molecular simulations of adsorption and phase transitions in nanopores. *Physical Review E*. 2001;64(1):011602. DOI: 10.1103/PhysRevE.64.011602

[50] Zhidong L, Dapeng C, Jianzhong W. Density-functional theory and Monte Carlo simulation for the surface structure and correlation functions of freely jointed Lennard-Jones polymeric fluids. *Journal of Chemical Physics*. 2005;122(17):174708–174709. DOI: 10.1063/1.1886685

[51] Libby B, Monson PA. Adsorption/desorption hysteresis in inkbottle pores: a density functional theory and Monte Carlo simulation study. *Langmuir*. 2004;20(10):4289–4294. DOI: 10.1021/la036100a

[52] Tang YP, Wu JZ. Modeling inhomogeneous van der Waals fluids using an analytical direct correlation function. *Physical Review E*. 2004;70(1): 011201. DOI: 10.1103/PhysRevE.70.011201

[53] Kong X, Gallegos A, Lu D, Liu Z, Wu J. A molecular theory for optimal blue energy extraction by electrical double layer expansion. *Physical Chemistry Chemical Physics*. 2015;17(37):23970–23976. DOI: 10.1039/c5cp03514g

[54] Peng B, Yu Y-X. A Density functional theory with a mean-field weight function: applications to surface tension, adsorption, and phase transition of a Lennard-Jones Fluid in a slit-like pore. *Journal of Physical Chemistry B*. 2008;112(48):15407–15416. DOI: 10.1021/jp805697p

[55] Ritter JA, Pan H, Balbuena PB. Adsorption of binary gas mixtures in heterogeneous carbon predicted by density functional theory: on the formation of adsorption azeotropes. *Langmuir*. 2010;26(17):13968–13975. DOI: 10.1021/la101865m

[56] Tang Y, Lu BCY. Analytical description of the Lennard-Jones fluid and its application. *Aiche Journal*. 1997;43(9):2215–2226. DOI: 10.1002/aic.690430908

[57] Rosenfeld Y. Relation between transport-coefficients and internal entropy of simple systems. *Physical Review A*. 1977;15(6):2545–2549. DOI: 10.1103/PhysRevA.15.2545

[58] Dzugutov M. A universal scaling law for atomic diffusion in condensed matter. *Nature*. 1996;381(6578):137–139. DOI: 10.1038/381137a0

[59] Mittal J, Errington JR, Truskett TM. Using available volume to predict fluid diffusivity in random media. *Physical Review E*. 2006;74(4): 040102. DOI: 10.1103/PhysRevE.74.040102

[60] Mittal J, Errington JR, Truskett TM. Relationships between self-diffusivity, packing fraction, and excess entropy in simple bulk and confined fluids. *Journal of Physical Chemistry B*. 2007;111(34):10054–10063. DOI: 10.1021/jp071369e

[61] Goel G, Krekelberg WP, Errington JR, Truskett TM. Tuning density profiles and mobility of inhomogeneous fluids. *Physical Review Letters*. 2008;100(10):106001. DOI: 10.1103/PhysRevLett.100.106001